

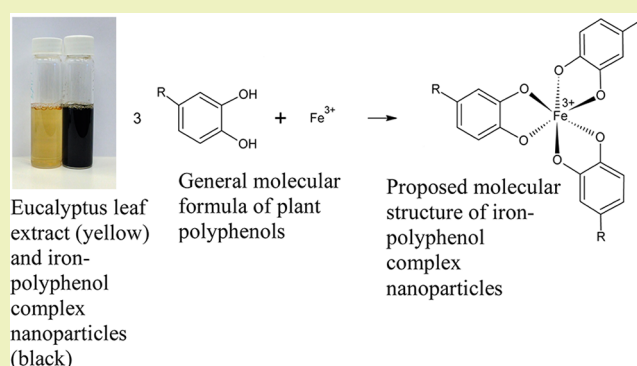
Iron Complex Nanoparticles Synthesized by Eucalyptus Leaves

Zhiqiang Wang*

†Centre for Environmental Risk Assessment and Remediation, University of South Australia, Mawson Lakes, SA 5095, Australia

ABSTRACT: Iron–polyphenol complex nanoparticles (Fe–P NPs) were synthesized using Eucalyptus leaves, which have potential for water purification and groundwater remediation due to their excellent adsorption–flocculation capacity. The Fe–P NPs have been characterized using transmission electron microscope (TEM), X-ray diffraction (XRD), and X-ray absorption spectroscopy (XAS). The result has shown that the Fe–P NPs are amorphous materials with sizes ranging from 40 to 60 nm. XAS investigation suggested that ferric ion is located in globular nanoparticles chelated by plant polyphenols. Maximum adsorption–flocculation capacity for acid black 194 with Fe–P NPs has been observed at 1.6 g per gram of Fe–P NPs at 25 °C.

KEYWORDS: Iron complex nanoparticles, Eucalyptus leaves, Plant polyphenols, XAFS, Dye adsorption–flocculation



■ INTRODUCTION

Plant polyphenols were referred to as vegetable tannins, which were used to convert animal skins into leather in ancient times. Today, several thousand plant polyphenols are known, encompassing a wide variety of molecules that contain at least one aromatic ring with one or more hydroxyl groups in addition to other substituents. They have been implicated in diverse functional roles, including antibiotic and antifeeding actions, protection against solar radiation, and antioxidation.¹ Recently, synthesis of iron nanoparticles using plant polyphenols have attracted much attention due to its environmental benignity, low cost, and simplicity. For example, iron nanoparticles have been synthesized with a polyphenol-rich green tea extract and performed as a catalyst in a Fenton-like process to degrade bromothymol blue, methylene blue, and methyl orange model dyes.² Chrysochoou et al. conducted a study for the treatment of Cr(VI)-contaminated soil at a Cr plating facility with green tea iron nanoparticles.³ However, the iron nanoparticle synthesized with plant extract showed different characters compared with zero-valent iron or iron oxide nanoparticles, which have not been explained exactly. It seems necessary to do more research to find out what they are.

For this reason, iron nanoparticles have been synthesized using *Eucalyptus tereticornis* leaves and characterized with TEM, XRD, and XAS to investigate their structures. The leaves of the Eucalyptus species contain mainly gallic acid, ellagic acid, hydrolyzable tannins, leucoanthocyanins, and flavonol glycosides, which can react with iron chloride solution to yield black complexes.⁴ Through characterization with TEM, it is found that interaction between Eucalyptus leaf polyphenols and iron chloride solution form iron–polyphenol nanoparticles (Fe–P NPs). The structural characterization of the Fe–P NPs was carried out using the X-ray absorption spectroscopy technique (XAS). The technique is sensitive to short-range order (a few

angstroms around the selected atom) and can be applied to disordered, amorphous, crystalline, and biological materials and to solutions as well. The adsorption–flocculation capacity and kinetics of Fe–P NPs have been tested through removing acid black 194 from water with UV–vis spectroscopy.

■ EXPERIMENTAL SECTION

Biosynthesis of Fe–P NPs. The plant leaf extract was prepared by heating 100 g of Eucalyptus leaves added to 500 mL of Milli-Q water at 80 °C for 1 h. After settling for 1 h, the extract was vacuum filtered. A solution of 0.10 M FeCl₃ was prepared by adding 16.23 g of FeCl₃ in 1.0 L of Milli-Q water, and subsequently, 0.1 M FeCl₃ solution was added to the leaf extract in a 2:1 ratio. The formation of green Fe NPs was marked by the appearance of a black color, and then Fe NPs were separated by centrifuging at 7000 rpm. The powders of Fe–P NPs were frozen at –20 °C and were dried in a freeze-dryer at –45 °C with the pressure at 10 Pa for 24 h.

Transmission Electron Microscopy. Morphological characteristics were analyzed with transmission electron microscopy (TEM) using Agilent FEI Technai 20. The sample was diluted 10 times.

X-ray Diffraction. XRD patterns of Fe–P NPs samples were obtained using a Philips PANalytical-Empeyrean instrument. The source consisted of Cu K α radiation ($\lambda = 1.54 \text{ \AA}$). Each sample was scanned within the 2θ range of 10–70°.

XAS Data Collection. X-ray absorption (XAS) experiments were performed at the Synchrotron Radiation Source at National University Singapore using the XAFCA beamline. The storage ring operates at 0.7 GeV and a typical current of 200 mA. A Si(111) double crystal was employed as a monochromator. Data were acquired in transmission mode. The ionization chamber was filled with an N₂ gas.

XAS Data analysis. XANES spectra were normalized to an edge jump of unity taking into account the atomic background after the

Received: June 13, 2013

Revised: July 15, 2013

Published: July 19, 2013

edge as it comes out from the EXAFS analysis. Prior removal of the background absorption was done by subtraction of a linear function extrapolated from the pre-edge region. XAS analysis has been performed by using the Athena and Artemis package⁵ that takes into account the multiple scattering theory. The method allows the direct comparison of the raw experimental data with a model theoretical signal.

Cyclic Voltammograms. Cyclic voltammetry analysis of the leaf extract was carried out in a BAS 100B/W electrochemical analyzer. A three-electrode system is employed: reference electrode (Ag/AgCl), working electrode (a glassy carbon disc 3.2 mm in diameter), and counter electrode (platinum wire). The scan rate was done in the potential range of -0.4 to 0.9 V versus the reference electrode at a scan rate of 50 mV s^{-1} .

Acid Black 194 Adsorption–Flocculation with Fe–P NPs. Acid black 194, with the molecular formula of $\text{C}_{20}\text{H}_{12}\text{N}_3\text{NaO}_7\text{S}$ (molecular weight 461.38) was used as adsorbate for the study of adsorption capacity and kinetics of Fe–P NPs. The dye was supplied by Sigma-Aldrich Australia. Adsorption capacity and kinetic experiments were performed in a set of 100 mL Erlenmeyer flasks, where a solution of dye (70 mL) with the initial concentration of 100 mg/L was placed. Different volumes of Fe–P NPs (0.2–1 mL) with a concentration of 0.0667 mol/L were added to the dye solution. After shaking, the mixtures were kept at 25°C for 24 h. The final concentration of dye in the solution was measured at 578 nm using a UV–vis spectrophotometer (Shimadzu 1601).

RESULTS AND DISCUSSION

The synthesized Fe–P NPs have no significant change in appearance and chemical characters after a one year storage. The pH is around 3 at a 2:1 ratio of FeCl_3 solution and plant extract. When the pH is adjusted to 7 and above, the black colloid changed to brown flocculation precipitate, which is assumed to yield $\text{Fe}(\text{OH})_3$. This phenomenon is consistent with Chrysochoou's observation,³ suggesting that the structure of the Fe–P NPs may have a structural similarity with $\text{Fe}(\text{OH})_3$.

In Figure 1, the TEM image shows that the Fe–P NPs were well dispersed in colloid with cubic particles ranging from 40 to

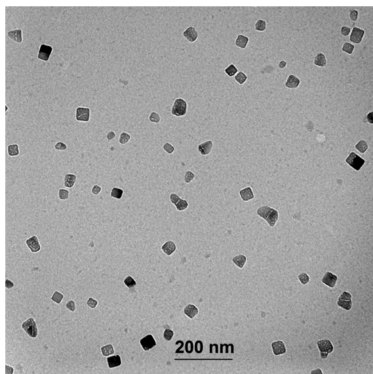


Figure 1. TEM image of the iron–polyphenol complex nanoparticles.

60 nm. The XRD patterns of the Fe–P NPs in Figure 2 lack distinct diffraction peaks, suggesting that the Fe–P NPs are amorphous.

The Fe K-edge XANES analysis is used in this work to determine the average Fe valence state in the Fe–P NPs sample. The energy position of the Fe K-edge in the Fe–P NPs sample is close to the edge position of the Fe^{3+} compounds (Figure 3), confirming that the iron in the sample is predominantly ferric ion. At the same time, we can clearly see that the derivative curve of Fe–P NPs is none of the model

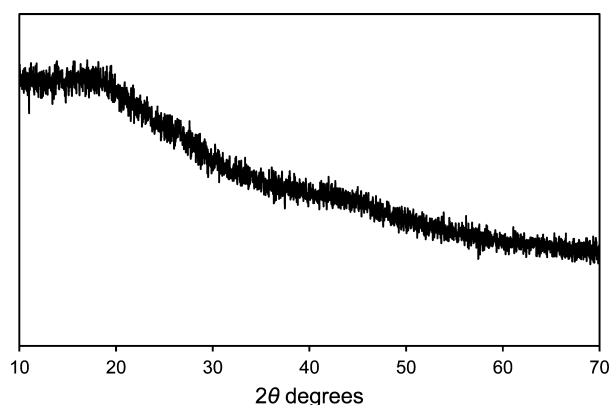


Figure 2. XRD spectrum of the iron–polyphenol complex nanoparticles.

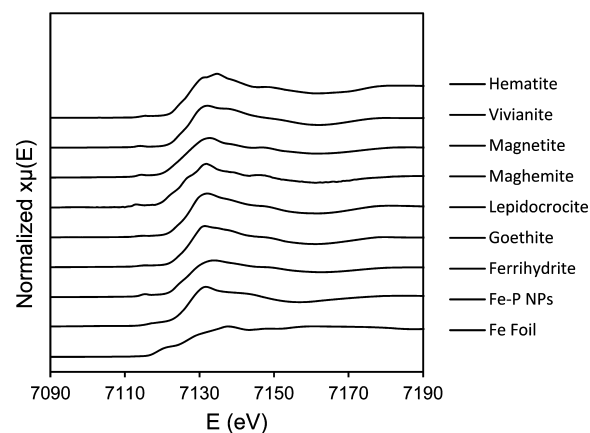


Figure 3. Experimental XANES spectra obtained at the Fe K-edge of Fe–P NPs and models.

samples (Figure 4), indicating that Fe–P NPs have different molecular structures from these model iron-containing materials.

Fe K-edge EXAFS analysis is used to directly probe the local structures around Fe cations in the Fe–P NPs. In the Fourier transform magnitude of the EXAFS spectrum (Figure 5), three distinct peaks are observed representing the contributions of

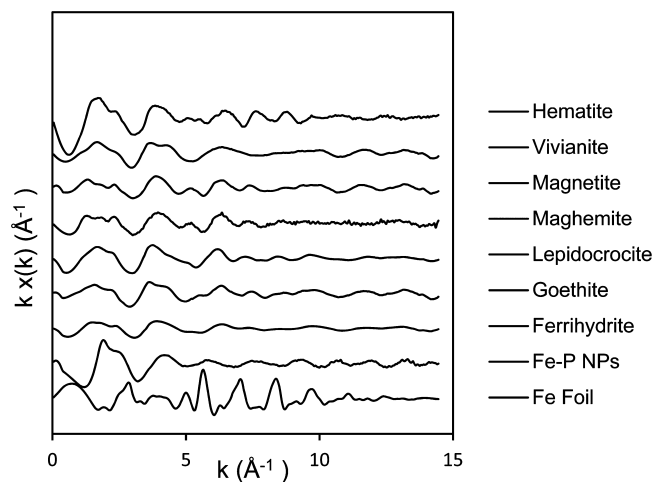


Figure 4. The k -extracted EXAFS signals of Fe–P NPs obtained at the Fe K-edge.

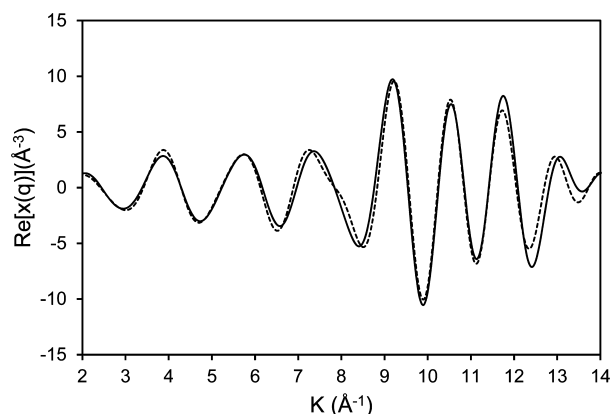


Figure 5. Fourier transform magnitude of k^2 -weighted EXAFS signals of the samples obtained at the Fe K-edge. Experimental (solid line); theoretical (dots).

photoelectron scattering on the nearest shells of neighbors around the Fe atom. A strong peak in the R range between 1.5 and 2.2 Å can be attributed to photoelectron backscattering on the nearest neighbors around Fe. The second peak between 2.2 and 2.5 Å and the third peak between 2.5 and 2.8 Å in the R range represents the contributions from more distant Fe coordination shells. Three variable parameters for each shell of neighbors are introduced in the model: shell coordination number (N), distance (R), and Debye–Waller factor (σ^2). A very good agreement between the model and experimental spectrum is found using the k range of 2–14 Å⁻¹, and the R range from 0 to 5 Å (Figures 5, 6). The list of best fit

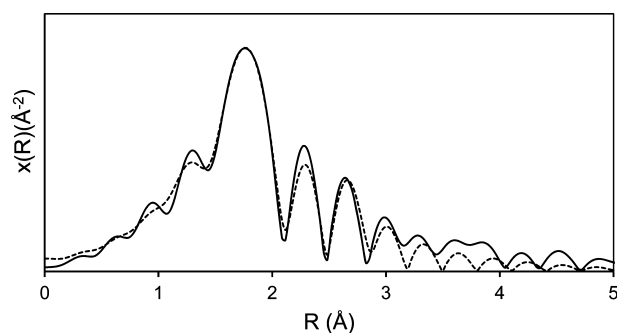


Figure 6. k^3 -weighted EXAFS signals of the Fe–P NPs obtained at the Fe K-edge. Experimental (solid line); theoretical (dots).

parameters is given in Table 1. Three oxygen atoms are identified in the fit of the Fe–O distance of 2.17 Å, and another three oxygen atoms are at 2.29 Å. Accordingly, a possible structure of the core the Fe–P NPs has been suggested in the table of contents and abstract graphics. In addition, two

Table 1. Structural Parameters R (Å), N , and σ (Å) Derived from the EXAFS Data Analysis of Fe–P NPs^a

bond	R (Å)	N	σ^2 (Å ²)
Fe–O	2.17	3	0.011
Fe–O	2.29	3	0.011
Fe–H	2.58	2	0.003
Fe–Fe	3.17	6	0.01

^a R , interatomic distance; N , coordination number; σ , Debye–Waller factor.

hydrogen atoms at 2.58 Å and six iron atoms at 3.17 Å can be found around the Fe–O shell as well. Relatively large Debye–Waller factors for the Fe coordination shell indicate a large disorder in the structure. Because polyphenol compounds are so structurally varied and the complexes formed are pH dependent, they may exhibit variable coordination modes.

The cyclic voltammogram was recorded to show its redox potential of Eucalyptus leaves extract. Figure 7 showed a broad

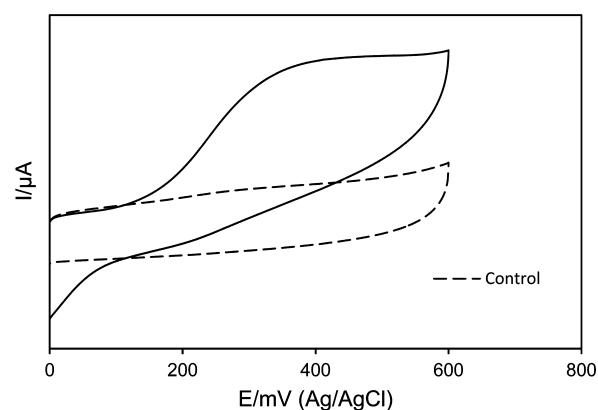


Figure 7. Cyclic voltammogram of extract of Eucalyptus leaves.

peak at +0.4 V due to various components of the leaves. The Fe³⁺/Fe²⁺ and Fe²⁺/Fe redox potentials are +0.77 V and –0.44 V, respectively. This indicated that Fe³⁺ can be reduced to Fe²⁺ by the leaves extract. However, Fe²⁺ is difficult to reduced to zero-valent iron by the leaves extract. Because polyphenol ligands strongly stabilize Fe³⁺ over Fe²⁺, the complexes of Fe²⁺ rapidly oxidize in the presence of O₂ to give Fe³⁺–polyphenol complexes, a process commonly referred to as autoxidation.⁶ Therefore, this explains why the FeCl₂ solution also yields a similar black nano iron colloid with plant leaves.⁷

Acid black 194 has been used to test the adsorption–flocculation capacity of the Fe–P NPs synthesized by Eucalyptus leaves. Acid black 194 is a kind of azo dye that is still in use in some counties, increasing the dangers in aspects of environment and human health. Maximum adsorption–flocculation capacity for acid black 194 with Fe–P NPs has been observed at 1.6 g acid black 194 per gram of Fe–P NPs at 25 °C. A kinetic study showed that removal rates of acid black 194 fitted well to the pseudo-first-order model (Figure 8).

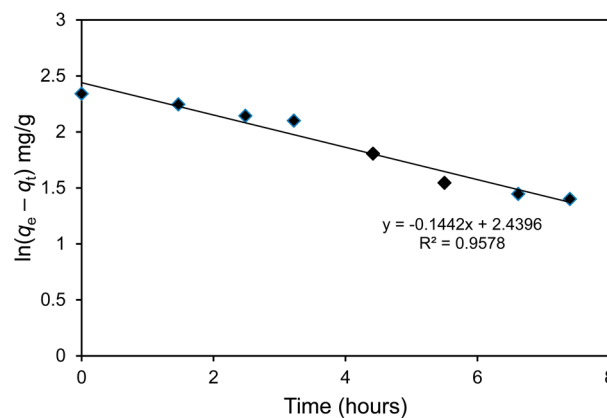


Figure 8. Pseudo-first-order kinetics for adsorption of acid black 194 dye on Fe–P NPs at 25 °C.

■ CONCLUSIONS

The structures of iron–polyphenol complex nanoparticles have been investigated. The Fe K-edge XANES and EXAFS structural information on iron in Fe–P NPs combined with TEM micrograph and XRD indicated that ferric ion is located in globular nanoparticles chelated by polyphenols. This nanomaterial presented excellent organic dye adsorption–flocculation capacity with maximum adsorption capacity of 1.6 g acid black 194 per gram of Fe–P NPs at 25 °C. In addition, polyphenol capping may reduce iron toxicity. Therefore, Fe–P NPs can be applied as an adsorption–flocculation agent in water purification and contaminated groundwater remediation.

■ AUTHOR INFORMATION

Corresponding Author

*Fax: 61-08-83025037. E-mail: zhiqiang.wang@mymail.unisa.edu.au.

Notes

The authors declare no competing financial interest.

■ ACKNOWLEDGMENTS

This work was supported by the Australian Postgraduate Awards.

■ REFERENCES

- (1) Quideau, S.; Deffieux, D.; Douat-Casassus, C.; Pouységu, L. Plant polyphenols: Chemical properties, biological activities, and synthesis. *Angew. Chem., Int. Ed.* **2011**, *50* (3), 586–621.
- (2) Hoag, G.; Collings, J.; Holcomb, J.; Hoag, Jessica; Nadagoud, M.; Varma, R. Degradation of bromothymol blue by ‘greener’ nano-scale zero-valent iron synthesized using tea polyphenols. *J. Mater. Chem.* **2009**, *19*, 8671–8677.
- (3) Chrysochoou, M.; Johnston, C. P.; Dahal, G. A comparative evaluation of hexavalent chromium treatment in contaminated soil by calcium polysulfide and green-tea nanoscale zero-valent iron. *J. Hazard. Mater.* **2012**, *201–202*, 33–42.
- (4) Hingston, F. Activity of polyphenolic constituents of leaves of Eucalyptus and other species in complexing and dissolving iron oxide. *Soil Res.* **1963**, *1* (1), 63–73.
- (5) Ravel, B.; Newville, M. ATHENA, ARTEMIS, HEPHAESTUS: Ddata analysis for X-ray absorption spectroscopy using IFEFFIT. *J. Synchrotron Radiat.* **2005**, *12* (4), 537–541.
- (6) Yoshino, M.; Murakami, K. Interaction of iron with polyphenolic compounds: Application to antioxidant characterization. *Anal. Biochem.* **1998**, *257* (1), 40–44.
- (7) Shahwan, T.; Abu Sirriah, S.; Nairat, M.; Boyacı, E.; Eroğlu, A. E.; Scott, T. B.; Hallam, K. R. Green synthesis of iron nanoparticles and their application as a Fenton-like catalyst for the degradation of aqueous cationic and anionic dyes. *Chem. Eng. J.* **2011**, *172* (1), 258–266.